Korean J. Chem. Eng., 32(5), 911-916 (2015)
DOI: 10.1007/s11814-014-0262-5

pISSN: 0256-1115
eISSN: 1975-7220

Low temperature synthesis of various transition metal oxides and their antibacterial activity against multidrug resistance bacterial pathogens

Ruddaraju Lakshmi Kalyani*, Jella Venkatraju, Pratap Kollu***, Nammi Hanumantha Rao****, and Sri Venkata Narayana Pammi****,†**

*Srinivasa Rao College of Pharmacy, P. M. Palem, Visakhapatnam, A.P-530041, India
**School of Nano Science and Technology, Chungnam National University, Daeduk Science Town, Daejeon 305-764, Korea
***DST-INSPIRE Faculty, Department of Metallurgical Engineering & Materials Science,
Indian Institute of Technology Bombay, Mumbai, India
****Advanced Analytical Laboratory, DST-PURSE Programme, Andhra University, Visakhapatnam 530003, India
(*Received 23 June 2014 • accepted 1 September 2014*)

Abstract−We report on the synthesis and characterization of various transition metal oxides, ZnO, CuO, TiO_2 and Fe_2O_3, using one pot wet chemical method at low temperature. The prepared metal oxide nanoparticles were characterized by X-ray diffraction (XRD), Raman and transmission electron microscopy (TEM) analyses. We tested antibacterial activity of as-prepared transition metal oxides against various multi-drug resistance bacterial pathogens such as *Escherichia coli*, *Bacillus subtilis*, *Pseudomonas aeruginosa*, and *Staphylococcus aureus*. XRD and TEM analyses revealed the average crystallite sizes were 18 nm, 20 nm, 10 nm and 22 nm for ZnO, CuO, TiO_2 and Fe_2O_3 nanoparticles, respectively. Further, the bacterial strains were grown in presence of different concentrations of four nanoparticles and it is evident from the results that ZnO, CuO nano particles showed greater bactericidal effect than nano-TiO_2 and nano-Fe_2O_3, though nano-TiO_2 possess less particle size than other fabricated metal oxide nanoparticles.

Keywords: Metal Oxides, Nanoparticles, Antibacterial Activity, Multi Drug Resistance

INTRODUCTION

Due to indiscriminate use of antibiotics, multi drug resistance (MDR) in human pathogens is one of the trending serious problems around the globe. It is latest huge challenge in pharmaceutical and biomedicine sectors [1]. Therefore, the goal is to discover novel strategies that directs ways to search for new antimicrobials. Nanotechnology offers possibilities to modify and develop salient properties of metals in form of nanoparticles by tailoring materials at the atomic or molecular level, thus obtaining novel characteristics with wide applications in diagnostics, biomarkers, cell labelling, contrast agents for biological imaging, antimicrobial agents, drug delivery systems and nanodrugs for treatment of various diseases [2,3]. Nanopaticles (NPs) exhibit entirely unique physical, chemical, and effective biological properties in various fields, including medicine, when compared to their bulk size counterparts [4,5]. Considering these unique properties, nanosized organic and inorganic particles are being generated owing to their potential application as antimicrobials. Amid these circumstances, inorganic particles have gained significant importance due to their ability to withstand adverse conditions as they are more stable at high temperatures and pressures [6].

Among various NPs, Silver nanoparticles have a high antimicrobial activity against a wide range of microbial pathogens. But, excess usage of silver NP's has adverse effects on the mankind, flora and fauna. They accumulate in skin (causing permanent decolorization of the skin, called argyria), kidney, brain and heart. Moreover, one of the dangers may be due to changes in microbial sensitivity to silver NPs [7]. Thus, metallic oxide powders can be used as powerful antimicrobial agents in this field [8]. The considerable antimicrobial activities of metal oxide NPs such as ZnO, Fe_2O_3, Fe_3O_4, MgO, CuO, TiO_2, SiO_2 and their selective toxicity to biological systems suggest their potential applications as therapeutics, diagnostics surgical devices and nano medicine based antimicrobial agents [9-13]. However, there have been many reports on the metal oxide NPs and their antibacterial activity which are synthesized at higher temperatures. High fabrication temperature of metal oxide NPs leads to low antibacterial activity due to their large crystallite size [5,7,8, 13]. In addition, in a large-scale synthesis scheme, high temperature is an expensive commodity. On the other hand, synthesis processes using green reducing agents allows synthesis of metal nanoparticles at room temperature but not to prepare metal oxide nanoparticles [14].

Our aim was to fabricate the transition metal oxide NPs (ZnO, CuO, TiO_2 and Fe_2O_3) at low temperatures (~100 °C) and to determine their antibacterial activity against multi drug resistance pathogenic bacteria such as *Escherichia coli, Staphylococcus aureus, Pseudomonas aeruginosa* and *Bacillus subtilis.*

EXPERIMENTAL SECTION

The selected (ZnO, CuO, TiO_2 and Fe_2O_3) transition metal oxide

†To whom correspondence should be addressed.
E-mail: sreepammi@gmail.com

NPs were prepared by simple and efficient wet chemical method at low temperatures (~100 °C). The detailed synthesis method is given in Supplementary Information. The morphological, structural and chemical composition of the prepared transition metal oxide NPs were analyzed with XRD (PANalytical), Raman spectroscopy (Horiba HR 8000, Excitation wavelength: 514.5 nm) and, TEM (JEOL-2100 F, HR) techniques.

1. Antibacterial Activity of Synthesized Metal Oxide NPs

The antibacterial activity of synthesized ZnO, CuO, TiO_2 and Fe_2O_3 NPs was tested against various MDR pathogens such as *E. coli*, *P. aeruginosa*, *B. subtilis* and *S. aureus*. The metal oxide NPs (ZnO, CuO, TiO_2 and Fe_2O_3 NPs) were tested to assess the minimum inhibitory concentration (MIC) required to hinder the progress of the four test pathogens elected in the study: Gram-positive (*B. subtilis* and *S. aureus*) and Gram-negative (*E. coli* and *P. aeruginosa*). For these, assorted dilutions of fabricated metal oxide NPs varying from 3.12 to 100 μg/ml were prepared with twofold symmetry. Four petri plates were taken for each NP (total of 16 plates) and 25 ml of MHA media was gushed into these petri plates and inoculated with each bacterial pathogen. Now the plates were whirled slowly for uniform dispensation of the inoculum and left at room temperature for 10 minutes with the lid shut. When the agar congealed, six pits (6 mm diameter) were made in each Petri plate with the aid of cork borer and each well was charged with manifold dilutions of metal oxide NPs (100 μg/ml, 50 μg/ml, 25 μg/ml, 12.5 μg/ml, 6.25 μg/ml, 3.12 μg/ml) solution. All the plates were incubated at 35 °C for 24 hrs. After the specified time period, the zone of inhibition formed at the minimum dilution for each pathogen was noted.

Depending on the preceding MIC values (see supplementary information) (Table 1-S.I), the dose 50 μg/ml was elected to test the antibacterial activity of metal oxide NPs (ZnO, CuO, TiO_2 and Fe_2O_3 NPs), antibiotic Rifampicin and DMSO solution. In short, four petri plates were taken and 25 ml of MHA media was spilled into these petri plates and inoculated with each bacterial patho-

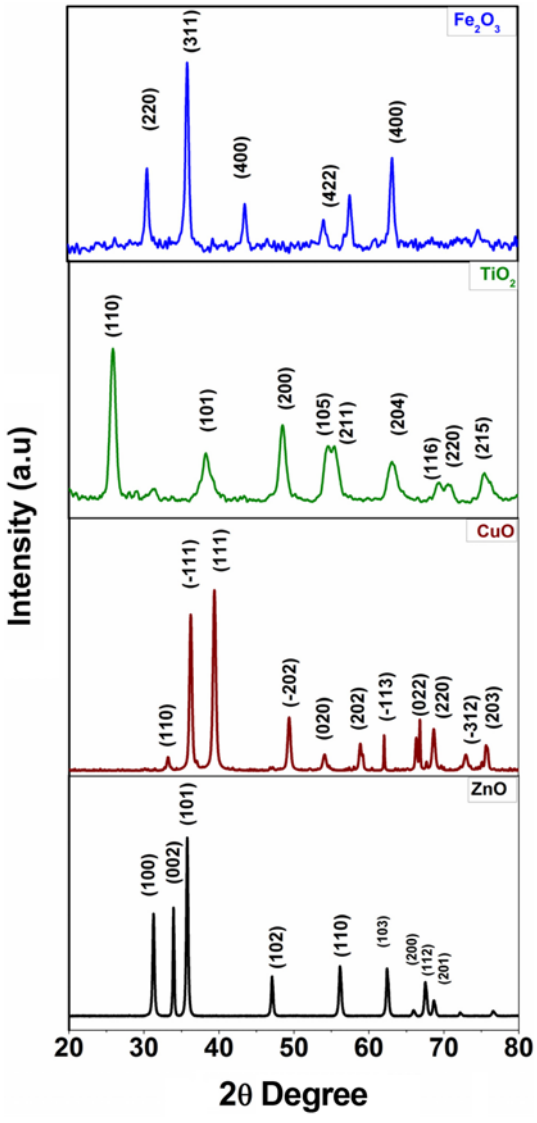

Fig. 1. XRD pattern of prepared metal oxide nanoparticles.

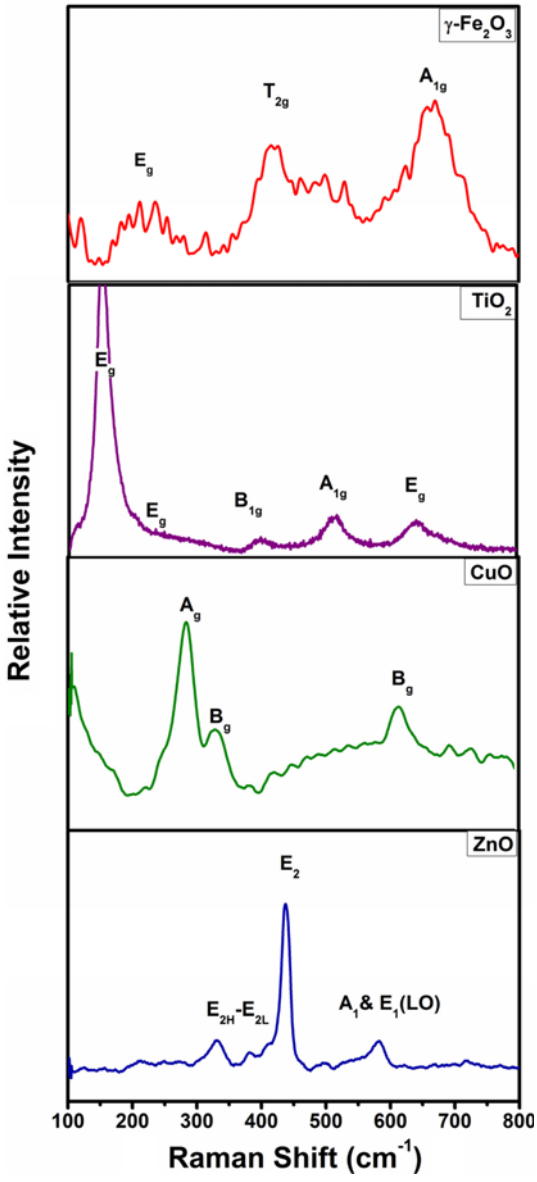

Fig. 2. Raman spectra of prepared metal oxide nanoparticles.

gen. When the agar solidified, four wells (6 mm diameter) were made in each petri plate with a cork borer and each well was filled with 50 µl of each metal oxide NP (50 µg/ml), metal oxide solution (0.1 M), antibiotic Rifampicin (50 µg/ml) and DMSO solution (50 µg/ml) in all the plates. All the plates were incubated at 35 °C for 24 h. After the stipulated time period, the zones formed were measured with a scale and recorded. Three replicates were preserved for each pathogen strain and the mean diameter value was expressed in millimeters.

RESULTS AND DISCUSSION

1. Characterization of Prepared Metal Oxide Nanoparticles

The typical XRD patterns of as prepared ZnO, CuO, TiO_2 and Fe_2O_3 NPs are shown in Fig. 1. The peak positions of samples exhibit hexagonal, monoclinic, anatase and rhombohedral phase of ZnO, CuO, $TiO_2$and Fe_2O_3, which was confirmed from the JCPDS Data card numbers 36-1451, 45-0397, 21-1272, and 01-089-5892, respectively. Furthermore, no metal or other impurity peaks were detected by XRD; thus the four metal oxides showed single-phase sample formation. The crystallite size of all four metal oxide NPs was also determined from X-ray line broadening using the Debye-Scherrer formula given as $D=0.9\lambda/\beta \cos \theta$, where D is the average crystallite size (A°), λ the X-ray wavelength used (nm), β the angular line width at half maximum intensity (radians) and θ the Braggs angle (degrees). The crystallite sizes were calculated to be 18 nm, 20 nm, 10 nm and 22 nm for ZnO, CuO, TiO_2 and Fe_2O_3 NPs, respectively.

The Raman-scattering spectra of the prepared metal oxides NPs are shown in Fig. 2. The main dominant sharp peak labelled as E_2 at 437 cm^{-1} was observed and is known as Raman active optical phonon mode, which is the characteristic of wurtzite hexagonal phase ZnO. Other peaks are also usually observed, i.e., the peak at 339 cm^{-1} is the second-order Raman spectrum, originating from the zone boundary phonons $3E_{2H}$-E_{2L} and at the peaks around 580 cm^{-1} were attributed to the superimposition of A_1 (LO) and E_1 (LO) [15]. From the Raman spectra of CuO NPs, it can be known that there are three Raman peaks at 289.3, 338.5 and 622.7 cm^{-1}, with the second one being the weakest and the third being broad. We can assign the peak at 289.3 cm^{-1} to the A_g mode and the peaks at 338.5 and 622.7 cm cm^{-1} to the B_g modes of single-phase CuO with a monoclinic structure [16]. From the Raman spectra of TiO_2 NPs it was concluded that the six allowed modes appear at 144 cm^{-1} (E_g), 197 cm^{-1} (E_g), 399 cm^{-1} (B_{1g}), 513 cm^{-1} (A_{1g}), and 639 cm^{-1} (E_g). We assigned and interpreted the Raman bands of the TiO_2 NPs using earlier results obtained for the bulk phase [17]. Raman spectra of synthesized γ-Fe_2O_3 NPs show small bands in between 200-

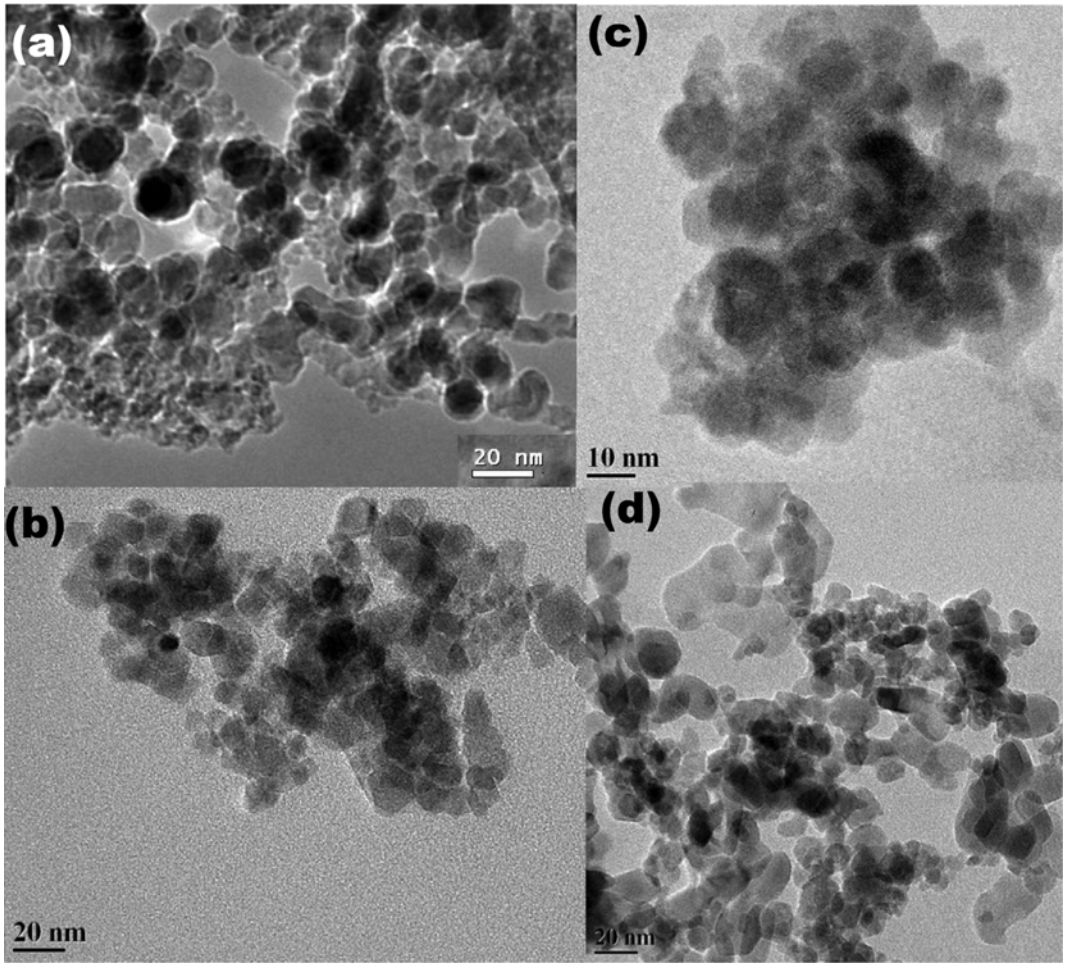

Fig. 3. TEM images of (a) ZnO (b) CuO (c) TiO_2 and (d) Fe_2O_3 nanoparticles.

300 cm^{-1} can be assigned as either A_{1g} mode or E_g mode of the α-Fe_2O_3 phase, respectively. This should be explained by the degradation of γ-Fe_2O_3 to α-Fe_2O_3 induced by the laser irradiation during Raman analysis. On the other hand, bands at 500 and 700 cm^{-1} were assigned to T_{2g} and A_{1g} modes with maghemite phase (γ-Fe_2O_3), which coincides with reported literature [18].

For further investigation, size and morphology of ZnO NPs were analyzed by TEM and it shows (Fig. 3(a)) small nanosized grains of spherical and hexagonal morphology with narrow size distribution ranging from 15-20 nm diameter. TiO_2 NPs (Fig. 3(b)) show the spherical and rhombic-shaped anatase NPs with diameters ranging from 7 to 10 nm. TEM analysis (Fig. 3(c)) demonstrated that nano CuO particles exhibited an approximate equi-axes shape with no sharp edges and the particle size was determined to be in the range 15-20 nm. Fig. 3(d) shows TEM image of γ-Fe_2O_3 NPs revealing nearly spherical shapes with average diameter of 20-25 nm. The average particle sizes determined by TEM images were very close to the crystallite size calculated from XRD results. Thus, the TEM results correlates well with XRD results.

2. Antibacterial Activity of Prepared Metal Oxide NPs

Each of two Gram positive (*B. subtilis* and *S. aureus)* and Gram negative (*E. coli* and *P. aeruginosa*) bacterial strains were examined

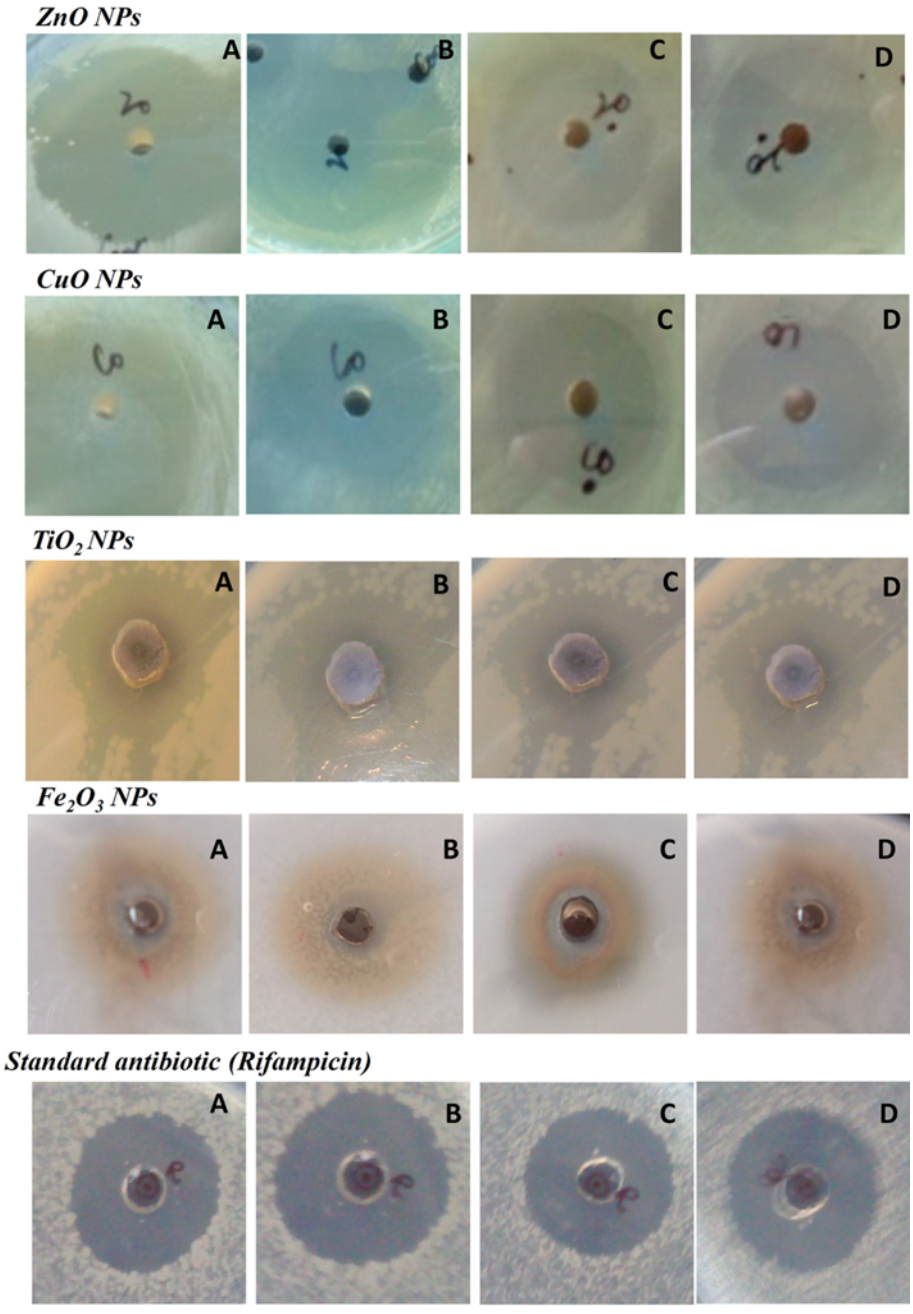

Fig. 4. Antibacterial activity of prepared transition metal oxide NPs along with standard antibiotic (Rifampicin) against *Escherichia coli* (A), *Bacillus subtilis* (B), *Pseudomonas aeruginosa* (C), and *Staphylococcus aureus* (D).

for their susceptibility to ZnO, CuO, TiO_2 and Fe_2O_3 NPs. Zone of inhibition values of different metal oxide NPs against tested bacterial pathogens is shown in Fig. 4. ZnO NPs showed maximum sensitivity of 33 mm against *B. subtilis* followed by 30 mm, 23 mm and 22 mm against *E. coli*, *S. aureus* and *P. aeruginosa,* respectively. On the other hand, CuO, TiO_2 and Fe_2O_3 NPs showed zones of inhibition of 25, 13 and 18 mm, respectively, against *B. subtilis*. In the case of *E. coli*, maximum growth inhibition zones were found to be the following: 28, 23, 15 and 16 mm for ZnO, CuO, TiO_2 and Fe_2O_3, respectively. It was concluded that the maximum zone of inhibition was exhibited by ZnO followed by CuO, Fe_2O_3 and TiO_2. However, ZnO and CuO showed superior antibacterial activity when compared to Fe_2O_3 and TiO_2 against all tested bacterial pathogens. Antibacterial activity results reveal ZnO and CuO NPs to be excellent antibacterial agents, whereas Fe_2O_3 showed moderate activity, and TiO_2 NPs shows poor activity when compared to standard antibiotic (Rifampicin). Note that, though TiO_2 NPs shows smaller in size when compared to other metal oxide NPs (from XRD and TEM analysis), it shows poorer antibacterial activity. Thus, there might be several factors involved other than size, such as, mixture concentration, surface properties of the NPs and the active oxygen generation and the particles of metal oxides [19,20].

S. aureus, E. coli, P. aeruginosa and *B. subtilis* were chosen as models to investigate the antibacterial activity of ZnO, CuO, TiO_2, Fe_2O_3 NPs, because they have demonstrated relatively high resistance to large number of antibiotics. We analyzed the MIC of these metal oxide NPs (Table 1-S.I) and we corroborated that the order of antibacterial activities of metal oxide NPs was shown at 3.12 μg/ml for ZnO & CuO, 6.25 μg/ml and 12.5 μg/ml for Fe_2O_3, TiO_2, respectively. ZnO NPs were found to be more sensitive to pathogens when compared to CuO Fe_2O_3, and TiO_2 NPs. The results of our investigation are supported by Baek and An and Wang et al., who surveyed that ZnO was the most toxic NP from a pool of ten NPs [8, 21]. Incidentally, Sawai et al. [22] also reported that nano-ZnO was most rugged against Gram-positive than Gram-negative bacteria, which was also shown in our study. The mechanism of inhibition for these metal oxide NPs might be as follows: The effect of nano-ZnO can be described on the basis of the oxygen species delivered on to the surface of ZnO, due to the inception of highly reactive species such as OH^-, H_2O_2 and O^{2-}. Since the hydroxyl radicals and superoxide are negatively charged particles, they cannot transfix into the cell membrane and must stay in unmediated association with the outer surface of the bacteria cell of the bacteria; however, H_2O_2 can penetrate into the cell [6,21] which roots to fatal damage of microorganisms [11,12]. The effect of nano-CuO might be due to release of copper ions that hitch to the negatively charged bacterial cell wall and rupture it, causing protein denaturation and cell death. Copper ions that enter into bacterial cells bind to DNA molecules and get cross-linked between the nucleic acid strands, resulting in a disorganized helical structure. In addition, copper ion uptake by the bacterial cells can also damage important biochemical processes [23]. Fe_2O_3 NPs generates Fe^{2+} which reacts with oxygen to create hydrogen peroxide. The H_2O_2 produced further reacts with ferrous irons through Fenton reaction and produces hydroxyl radicals which are known to damage biological macromolecules [24]. In case of TiO_2 NPs, antibacterial activity might be due to the generation of O^{-2} species. It is well known that TiO_2 has photo catalytic properties, and it has been reported that TiO_2 has significant antimicrobial properties under UV light conditions. In addition there is no distinct mechanism reported for TiO_2 NPs under dark light conditions [25]. We concluded that concentration affected cell death, with ROS being the predominant mechanism. However, previous studies have shown that the smaller the particle size, the greater the efficacy in inhibiting the growth of bacteria. But, in case of metal oxides synthesized at almost equal temperature in our experiments, though TiO_2 NPs showed smaller size (from XRD and TEM analysis) than the other synthesized NPs (ZnO, CuO, Fe_2O_3), it shows least inhibitory effect when compared to other NPs. The release of metal ions is a key factor for the antimicrobial activities of metal oxide NPs. Among all the four tested NPs, ZnO NPs showed the highest antimicrobial activity. Nevertheless, it is also crucial to know the vital physicochemical properties that govern antibacterial activity and cytotoxicity of these metal oxide NPs to mammalian cells. In this instance, it is essential to assess the task of size, shape, morphology, and electronic properties on cytotoxicity as the metal oxide NPs are well known to possess wide biomedical applications [26]. The ruling factor for risk appraisal relying on cytotoxicity encompasses the framework of NPs, solubility and their biological interactions. These results help in providing a background for the design of safe metal oxide NP products to kill bacterial pathogens.

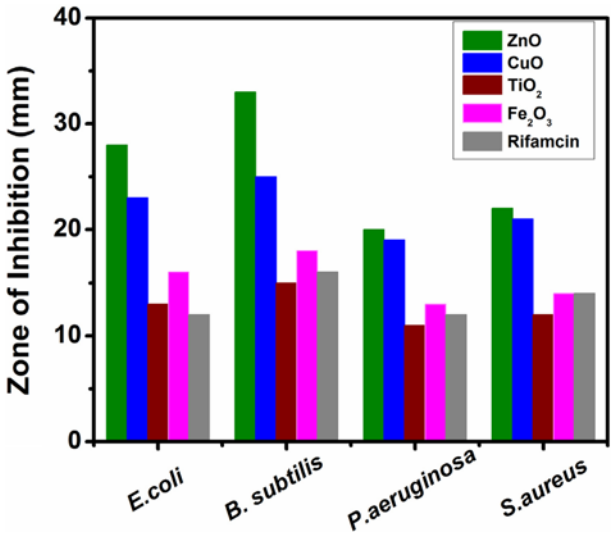

Fig. 5. Comparison of values of zone of inhibition of prepared metal oxide NPs including standard antibiotic (rifampicin) against multi drug resistance bacteria.

CONCLUSIONS

ZnO, CuO, TiO_2 and Fe_2O_3 nanosized particles were synthesized by one pot chemical method at low temperatures. XRD and TEM results showed that TiO_2 nanoparticles were smallest (10 nm) compared to ZnO (15 nm) CuO (20 nm), and Fe_2O_3 (22 nm). Also, the antibacterial activity of all these four synthesized nanomaterials was collated and shown to be in disparity massively. Antimicrobial activity generally appears to increase with increase in surface-

to-volume ratio due to decrease in particle size of nanoparticles. But in this case, though TiO_2 is smaller, ZnO nanoparticles showed excellent bactericidal potential, while TiO_2 NPs had the least bactericidal activity. Our results indicate that nanomaterials were most effective against both the Gram-positive and Gram-negative bacterial strains.

ACKNOWLEDGEMENTS

We thank the DST-PURSE Programme for the financial assistance and Advanced Analytical Laboratory, Andhra University, for their support in carrying out in this research work regarding XRD analysis. Authors are also grateful to SAIF, IIT Bombay for TEM and Raman characterization.

REFERENCES

1. F. C. Tenover, *Am. J. Medicine,* **119**, S3 (2006).
2. P. D. Marcato and N. Duran, *J. Nanosci. Nanotechnol.*, **8**, 2216 (2008).
3. R. Singh and N. H. Singh, *J. Biomed. Nanotechnol.,* **7**, 489 (2011).
4. W. Rizwan, K. Young-Soon, M. Amrita, Y. Soon-II and H.-S. Shin, *J. Nanoscale Res. Lett.*, **5**(10), 1675 (2010).
5. G. Priyanka, P. Brian, W. B. David, H. Wenjie, P. J. William and J. A. Anne, *J. Bio. Eng.*, **3**(9), 1 (2009).
6. J. Sawai, *J. Microbiol. Methods*, **54**, 177 (2003).
7. M. Soltani, M. Ghodratnema, H. Ahari, H. A. Ebrahimzadeh Mousavi, M. Atee, F. Dastmalchi and J. Rahmanya, *International Journal of Veterinary Research*, **3**(2), 137 (2009).
8. Z. Wang, Y. Lee and B. Wu, *Chemosphere*, **80**, 525 (2010).
9. J. Mohsen and B. Zahra, *Afr. J. Biotechnol.*, **7**(25), 4926 (2008).
10. K. Sobha, K. Surendranath, V. Meena, K. T. Jwala, N. Swetha and K. S. M. Latha, *J. Biotechnol. Mol. Bio. Rev.*, **5**(1), 1 (2010).
11. K. A. Laura, Y. L. Delina and J. J. A. Pedro, *J. Water Res.*, **40**, 3527 (2006).
12. K. M. Reddy, F. Kevin, B. Jason, G. W. Denise, H. Cory and P. Alex, *J. Appl. Phys. Lett.*, **90**(21), 1 (2007).
13. M. A. Vargas-Reus, K. Memarzadeh, J. Huang, G. G. Ren and R. P. Allaker, *International Journal of Antimicrobial Agents*, **40**, 135 (2012).
14. S. Iravani, *Green Chem.*, **13**, 2638 (2011).
15. S. Bai, J. Hu, D. Li, R. Luo, A. Chena and C. C. Liub, *J. Mater. Chem.*, **21**, 12288 (2011).
16. J. F. Xu, W. Ji, X. Shen and S. H. Tang, *J. Solid State Chem.*, **147**, 516 (1999).
17. T. Ohsaka, *J. Phys. Soc. Jpn.*, **48**, 1661 (1980).
18. D. Thierry, D. Persson, C. Legraph, D. Delichere, S. Joiret, C. Pallota and A. Hugot-Legoff, *J. Electrochem. Soc.*, **135**, 305 (1988).
19. S. Makhluf, R. Dror, Y. Nitzan, Y. Abramovich, R. Jelnek and A. Gedanken, *Adv. Funct. Mater.*, **15**, 1708 (2005).
20. L. Zhang, Y. Jiang, Y. Ding, N. Daskalakis, L. Jeuken, M. Povey, A. J. O'Neill and D. W. York, *Progress in Natural Science*, **18**, 939 (2008).
21. Y. Baek and Y. An, *Sci. Total Environ.*, **409**, 1603 (2011).
22. J. Sawai and T. Yoshikawa, *J. Appl. Microbiol.*, **96**, 803 (2004).
23. G. Ren, D. Hu, E. W. Cheng, M. A. Vargas-Reus, P. Reip and R. P. Allaker, *Int. J. Antimicrob. Agents*, **33**(6), 587 (2009).
24. C. R. Keenan and D. L. Sedlak, *Environ. Technol.*, **42**(4), 1262 (2008).
25. M. Allahverdiyev, E. S. Abamor, M. Bagirova and M. Rafailovich, *Future Microbiology*, **6**, 933 (2011).
26. R. Brayner, *Nano Today*, **3**, 48 (2008).

Supporting Information

Low temperature synthesis of various transition metal oxides and their antibacterial activity against multidrug resistance bacterial pathogens

Ruddaraju Lakshmi Kalyani*, Jella Venkatraju, Pratap Kollu***, Nammi Hanumantha Rao****, and Sri Venkata Narayana Pammi****,†**

*Srinivasa Rao College of Pharmacy, P. M. Palem, Visakhapatnam, A.P-530041, India
**School of Nano Science and Technology, Chungnam National University, Daeduk Science Town, Daejeon 305-764, Korea
***DST-INSPIRE Faculty, Department of Metallurgical Engineering & Materials Science,
Indian Institute of Technology Bombay, Mumbai, India
****Advanced Analytical Laboratory, DST-PURSE Programme, Andhra University, Visakhapatnam 530003, India
(*Received 23 June 2014 • accepted 1 September 2014*)

Synthesis and Characterization of Zinc Oxide NPs:

ZnO NPs were synthesized by simple wet chemical method. ZnO NPs were grown from a solution of analytical grade with high purity of Zn $(CH_3COO)_2$ (Zinc Acetate) a Zn^{++} ion source and urea in an alkaline solution of ammonia. Aqueous solutions of analytical grade with high purity 0.2 M zinc acetate (Zn $(CH_3COO)_2$), 0.6 M urea $(CO(NH_2)_2)$, and complexing agent (ammonia, 70% hydrazine hydrate or 0.2×2/3 M tri-sodium citrate) were used to prepare ZnO NPs. Initially, 10 ml of zinc acetate solution and 10 ml of tri-sodium citrate were taken in a 100 ml beaker, and stirred for several minutes till the solution becomes clear and homogenous. Under continuous stirring, 10 ml urea solution was introduced in to the above solution and finally made up to volume (50 ml) with de-ionized water. The pH of the resultant solution was adjusted to about 10 by adding ammonia solution. The solution was continuously stirred at a constant speed during the growth time with the help of AC motor. The bath temperature was raised to a maximum of 80±5 °C from room temperature using temperature controller. The ZnO NPs were washed with deionized water and methanol ultrasonically to remove the loosely adhered ZnO particles and finally dried in vacuum at 100 °C for 24 hr. to evaporate solvents in ZnO nano powder.

Synthesis and Characterization of Titanium Oxide (TiO_2) NPs

In a typical process, 5 ml of titanium iso-propoxide was dissolved in 5 ml of anhydrous alcohol, and ultrasonically dispersed to produce a mixture. Meanwhile, 5 ml of water and 1 ml of HNO_3 (65%) were added to another 20 ml of absolute ethanol in turn to form an ethanol-nitric acid-water mixture solution. The titanium iso-propoxide - C_2H_5OH solution was slowly added drop wise to the ethanol nitric acid-water solution under vigorous stirring for 15 min to carry out the process of hydrolysis. Ultimately, a semitransparent solution was achieved after continuous stirring for 1 h, subsequently; the solution was conducted by which the temperature was raised from 25 to 80 °C at the end of the reaction. The obtained precipitates were separated by filtering, and washed for several times with de-ionized water and anhydrous alcohol, and dried at 100 °C in the air for about 24 h and then grounded to produce dry nano-TiO_2 powder.

Synthesis and Characterization of Copper Oxide (CuO) NPs

CuO NPs were synthesized by simple and efficient chemical bath deposition method. CuO NPs were grown from a solution of analytical grade with high purity of, Cu $(NO_3)_2$, (Copper nitrate) a Cu^{++} ion source and urea in an alkaline solution of Triethylenediamine (DABCO). Aqueous solutions of analytical grade with high purity 0.2 M Copper nitrate (Cu $(NO_3)_2$), 0.6 M urea $(CO(NH_2)_2)$, and complexing agent (Triethylenediamine, 70% hydrazine hydrate or 0.2×2/3 M tri-sodium citrate) were used to prepare CuO NPs. Initially, 10 ml of Copper nitrate solution and 10 ml of tri-sodium citrate were taken in a 100 ml beaker, and stirred for several minutes till the solution becomes clear and homogenous. Under continuous stirring, 10 ml urea solution was introduced in to the above solution and finally made up to volume (50 ml) with de-ionized water. The pH of the resultant solution was adjusted to about 10 by adding ammonia solution. The solution was continuously stirred at a constant speed during the growth time with the help of AC motor. The bath temperature was raised to a maximum of 80±5 °C from room temperature using temperature controller. The CuO NPs were washed with deionized water and methanol ultrasonically to remove the loosely adhered CuO particles and finally dried in vacuum at 100 °C for 24 h. to evaporate solvents in CuO nano powder.

Synthesis and Characterization of Iron Oxide NPs:

$Fe(NO_3)_3{\cdot}9H_2O$, poly ethylene glycol (PEG2000) and potassium chloride (KCl) were analytical grade. Double distilled water was used in preparation. The preparation procedure was as follow: First, 0.006 mol Fe $(NO_3)_3{\cdot}9H_2O$ was dissolved in 100 ml aqueous solution of PEG2000 with a NO_3-/PEG2000 molar ratio of 1. Then, the desired amount of KCl was added to the above solution and the resulting transparent solution was thoroughly stirred by a magnetic mixer at 70 °C until a homogeneous sol-like solution was formed. Afterwards, the sol-like solution was dried at 100 °C for 24 h. The obtained gel was placed in a silica crucible and heated in air until the gel was ignited. The as-burned powders were boiled in deionized water to remove the salt. Final product was obtained after filtrating, washing with deionized water and ethanol, drying at 80 °C for 2 h.

Table 1. Antibacterial activity of prepared metal oxide NPs (3.12-100 μg/ml) against various multidrug resistance bacteria

Concentration of ZnO NPs						
Bacterial pathogens	100 (μg/ml)	50 (μg/ml)	25 (μg/ml)	12.5 (μg/ml)	6.25 (μg/ml)	3.12 (μg/ml)
E. coli	30	28	25	20	20	18
B. subtilis	33	30	27	24	23	20
P. aeruginosa	22	20	18	16	13	12
S. aureus	23	22	20	17	16	14
Concentration of CuO NPs						
Bacterial pathogens	100 (μg/ml)	50 (μg/ml)	25 (μg/ml)	12.5 (μg/ml)	6.25 (μg/ml)	3.12 (μg/ml)
E. coli	25	23	17	15	13	12
B. subtilis	28	25	23	22	20	18
P. aeruginosa	23	19	19	17	16	14
S. aureus	24	21	22	20	18	17
Concentration of TiO_2 NPs						
Bacterial pathogens	100 (μg/ml)	50 (μg/ml)	25 (μg/ml)	12.5 (μg/ml)	6.25 (μg/ml)	3.12 (μg/ml)
E. coli	18	15	11	-	-	-
B. subtilis	15	13	9	-	-	-
P. aeruginosa	12	11	6	-	-	-
S. aureus	13	12	8	-	-	-
Concentration of Fe_2O_3 NPs						
Bacterial pathogens	100 (μg/ml)	50 (μg/ml)	25 (μg/ml)	12.5 (μg/ml)	6.25 (μg/ml)	3.12 (μg/ml)
E. coli	19	16	13	8	-	-
B. subtilis	20	18	15	11	-	-
P. aeruginosa	15	13	9	6	-	-
S. aureus	17	14	10	7	-	-

Table 2. Zone of Inhibition values of prepared metal oxide nanoparticles and standard antibiotic Rifampicin with dose of 50 μg/ml against various multidrug resistance bacteria

Bacterial pathogens	ZnO	CuO	TiO_2	Fe_2O_3	Rifampicin
E. coli	28	23	15	16	16
B. subtilis	33	25	13	18	14
P. aeruginosa	20	19	11	13	12
S. aureus	22	21	12	14	14